

Coupled Cluster Treatment of the Shastry-Sutherland Antiferromagnet

R. Darradi^a, J. Richter^a, and D. J. J. Farnell^b

^a*Institut für Theoretische Physik,
Otto-von-Guericke Universität Magdeburg,
P.O.B. 4120, 39016 Magdeburg, Germany*

^b*Unit Of Ophthalmology, Department of Medicine,
University Clinical Departments,
Daulby Street, University of Liverpool,
Liverpool L69 3GA, United Kingdom*

(Dated: December 2, 2024)

We consider the zero-temperature properties of the spin-half two-dimensional Shastry-Sutherland antiferromagnet by using a high-order coupled cluster method (CCM) treatment. We find that this model demonstrates various groundstate phases (Néel, magnetically disordered, orthogonal dimer), and we make predictions for the positions of the phase transition points. In particular, we find that orthogonal-dimer state becomes the groundstate at $J_2^d/J_1 \sim 1.477$. For the critical point J_2^c/J_1 where the semi-classical Néel order disappears we obtain a significantly lower value than J_2^d/J_1 , namely, J_2^c/J_1 in the range [1.14, 1.39]. We therefore conclude that an intermediate phase exists between the Néel and the dimer phases. An analysis of the energy of a competing spiral phase yields clear evidence that the spiral phase does not become the groundstate for any value of J_2 . The intermediate phase is therefore magnetically disordered but may exhibit plaquette or columnar dimer ordering.

I. INTRODUCTION

The study of two-dimensional (2D) quantum magnetism has attracted much experimental and theoretical attention over many years. In 2D antiferromagnets at zero temperature the competition between interactions and quantum fluctuations is well balanced and one sees magnetic long-range order (LRO) as well as magnetic disorder, dependent on details of the lattice^{1,2,3,4}. In particular, frustration may lead to the breakdown of semi-classical Néel LRO in 2D quantum antiferromagnets. Much research activity in this area has been focused on frustrated spin-half Heisenberg antiferromagnets on the square lattice, such as the J_1 - J_2 model with competing antiferromagnetic nearest-neighbor J_1 and next-nearest-neighbor J_2 bonds (see, e.g., Refs.^{5,6,7,8,9,10,11} and references therein), where a quantum paramagnetic phase near $J_2 \sim 0.5J_1$ is observed the nature of which is still under discussion. Another canonical model is the Shastry-Sutherland antiferromagnet introduced in the eighties¹², which has special arrangement of frustrating next-nearest-neighbor J_2 bonds on the square lattice, cf. Fig.1. We note that for bonds of equal strength, i.e., $J_1 = J_2$, the Shastry-Sutherland model is equivalent to a Heisenberg model on one of the eleven uniform Archimedean lattices⁴. Although the initial motivation to study this special frustrated square-lattice antiferromagnet is related to the existence of a simple singlet-product eigenstate (which becomes the groundstate (GS) for strong frustration), the renewed interest in the last years was stimulated by the discovering of the new quantum phase in $\text{SrCu}(\text{BO}_3)_2$ ^{13,14} which can be understood in terms of the Shastry-Sutherland model. Although the GS of this model in the limit of small frustration J_2 and

large J_2 is well understood, the GS phase at moderate J_2 is still a matter of discussion.

In this paper, we study the GS phase diagram for spin half Shastry-Sutherland model using a high-order coupled cluster treatment. The coupled cluster method (CCM) is one of the most universal and powerful methods of quantum many-body theory. The CCM has previously been applied to various quantum spin systems with much success^{8,15,16,17,18,19,20,21,22,23}. We mention that one particular advantage of this approach consists in applicability to strongly frustrated quantum spin systems in any dimension, where some other methods, such as, e.g., the quantum Monte Carlo method fail.

II. THE MODEL

The Shastry-Sutherland model is a spin- $\frac{1}{2}$ Heisenberg model on a square lattice with antiferromagnetic nearest-neighbor bonds J_1 and with one antiferromagnetic diagonal bond J_2 in each second square (see Fig.1). It is described by the Hamiltonian

$$H = J_1 \sum_{\langle i,j \rangle} \mathbf{s}_i \cdot \mathbf{s}_j + J_2 \sum_{\{i,k\}} \mathbf{s}_i \cdot \mathbf{s}_k, \quad (1)$$

where the operators \mathbf{s}_i represent spin-half operators, i.e., $\mathbf{s}_i = \mathbf{s}(\mathbf{s} + 1)$ with $s = 1/2$. The sums over $\langle i,j \rangle$ and $\{i,k\}$ run over all nearest-neighbor bonds and over some of the next-nearest-neighbor bonds according to the pattern shown in Fig. 1. Due to the special arrangement of the J_2 bonds the unit cell contains four sites. Therefore it is convenient to split the square lattice into four equivalent sublattices A, C, B and D as shown in Fig.(1). It

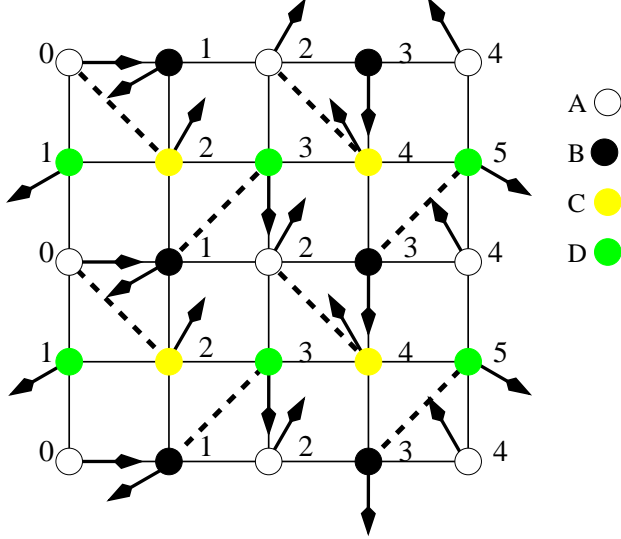


FIG. 1: Illustration of the classical spiral state for Shastry-Sutherland model of Eq. (1), with nearest-neighbor bonds J_1 (solid lines) and next-nearest-neighbor bonds J_2 (dashed lines). The spin orientations at A; C and B; D lattice sites are defined by the angles $\theta = n\phi$ and $\theta = n\phi + \pi$, respectively, where $n = 0, 1, 2, \dots$, and ϕ is the characteristic angle of the spiral state. The state is shown for $\phi = \pi/6$ and $n = 0, 1 \dots 5$.

what follows we set $J_1 = 1$ and consider $J_2 > 0$ as the parameter of the model.

The classical (i.e., $s \rightarrow \infty$) GS of the Shastry-Sutherland model is the collinear Néel state for $J_2/J_1 \leq 1$, but a noncollinear spiral state for $J_2/J_1 > 1$ (see Fig.1 and Refs. 24,25) with a characteristic pitch angle ϕ given by

$$\phi = \begin{cases} 0 & J_2 \leq J_1 \\ \arccos(-J_1/J_2) & J_2 > J_1 \end{cases} \quad (2)$$

We note that for $\phi = 0$ the spiral state becomes the collinear Néel state classically. The transition from the collinear Néel to noncollinear spiral state is of second order and takes place at $J_2/J_1 = 1$. We note further that there are only two different angles between interacting spins, namely, $\phi + \pi$ for the J_1 couplings and -2ϕ for the J_2 couplings.

The quantum $s = 1/2$ version of the model has been treated previously by various methods like Schwinger boson mean-field theory²⁴, exact diagonalization^{14,26}, series expansions^{25,27,28,29}, renormalization group³⁰ and also by a gauge-theoretical approach³¹. A recent review can be found in Ref. 32. From these studies one knows that for small $J_2 \leq J_1$ the physics of the quantum model is similar to that of the classical model, i.e., we have semi-classical Néel order. Furthermore, one knows already from the early work of Shastry and Sutherland¹² that for large J_2 the quantum GS is a rotationally invariant product state of local pair singlets (so-called orthogonal-dimer state) $|\Psi\rangle_{\text{dimer}} = \prod_{\{i,j\} J_2} [|\uparrow_i\rangle|\downarrow_j\rangle - |\downarrow_i\rangle|\uparrow_j\rangle]/\sqrt{2}$, where

i and j correspond to those sites which cover the J_2 bonds. The energy per site of this orthogonal-dimer state is $E_{\text{dimer}}/N = -3J_2/8$. It becomes the GS at around $J_2^c \approx (1.44 \dots 1.49)J_1$ (see Table 2 in Ref. 32). Note that such an orthogonal-dimer state can be observed also in corresponding one-dimensional and three-dimensional models^{33,34,35}. The nature of the transition between the semi-classical Néel state and the orthogonal-dimer phase is still a matter of controversial discussion. In the region $1.2J_1 \lesssim J_2 \lesssim 1.45J_1$ the main question is whether the system has an intermediate phase. A direct transition between the Néel phase and the orthogonal-dimer phase is favored in Refs. 14,27,28,30, whereas in Refs. 24,25,26,31 the existence of an intermediate phase is found. However, concerning the nature of this intermediate phase controversial results are reported, as candidates for the intermediate phase are quantum spiral phases^{24,31} or a plaquette or columnar singlet phases^{25,26} discussed.

To contribute to the solution of this open problem the CCM is an appropriate method, since it is one of the methods which can deal with spiral phases in quantum spin models.^{19,21,36}

III. THE COUPLED CLUSTER METHOD

The CCM formalism is now briefly considered, although the interested reader is referred to Refs. 16,18,19,20,22 for further details. The starting point for the CCM calculation is the choice of a normalized reference or model state $|\Phi\rangle$. For spin systems, an appropriate choice for the CCM model state $|\Phi\rangle$ is often a classical spin state, in which the most general situation is that each spin can point in an arbitrary direction. In order to treat the Shastry-Sutherland model using the CCM, we choose the Néel state and the spiral state in Fig.(1) to be our model states. We note that we do not choose the classical result for the pitch angle ϕ but we consider it rather as a free parameter in the CCM calculation.

To treat each site equivalently we perform a rotation of the local axis of the spins such that all spins in the reference state align in the same direction, namely along the negative z axis, such that we have $|\Phi\rangle = |\downarrow\rangle|\downarrow\rangle|\downarrow\rangle|\downarrow\rangle\dots$. We define a set of multi-spin creation operators $C_I^+ = s_r^+, s_r^+ s_l^+, s_r^+ s_l^+ s_m^+, \dots$

The choice of the C_I^+ ensures that $\langle\Phi|C_I^+ = 0 = C_I|\Phi\rangle$, where C_I is the Hermitian adjoint of C_I^+ .

In order to make the spin s_i to be aligned along the negative z axis one has to perform a rotation of the respective spin by an appropriate angle δ_i . This rotation is equivalent to the canonical transformations,

$$\begin{aligned} s_i^x &= \cos \delta_i s_i^x + \sin \delta_i s_i^z \\ s_i^y &= s_i^y \\ s_i^z &= -\sin \delta_i s_i^x + \cos \delta_i s_i^z. \end{aligned} \quad (3)$$

Using this transformation the Hamiltonian (1) is then

rewritten as

$$\begin{aligned}
H = & J_1 \sum_{\langle i,j \rangle}^N \left(\frac{1}{2} \sin \varphi_{i,j} [\hat{s}_i^+ \hat{s}_j^z - \hat{s}_i^z \hat{s}_j^+ + \hat{s}_i^- \hat{s}_j^z - \hat{s}_i^z \hat{s}_j^-] \right. \\
& + \cos \varphi_{i,j} \hat{s}_i^z \hat{s}_j^z + \frac{1}{4} (\cos \varphi_{i,j} + 1) [\hat{s}_i^+ \hat{s}_j^- + \hat{s}_i^- \hat{s}_j^+] \\
& \left. + \frac{1}{4} (\cos \varphi_{i,j} - 1) [\hat{s}_i^+ \hat{s}_j^+ + \hat{s}_i^- \hat{s}_j^-] \right) \\
& + J_2 \sum_{\{i,k\}}^N \left(\frac{1}{2} \sin \varphi_{i,k} [\hat{s}_i^+ \hat{s}_k^z - \hat{s}_i^z \hat{s}_k^+ + \hat{s}_i^- \hat{s}_k^z - \hat{s}_i^z \hat{s}_k^-] \right. \\
& + \cos \varphi_{i,k} \hat{s}_i^z \hat{s}_k^z + \frac{1}{4} (\cos \varphi_{i,k} + 1) [\hat{s}_i^+ \hat{s}_k^- + \hat{s}_i^- \hat{s}_k^+] \\
& \left. + \frac{1}{4} (\cos \varphi_{i,k} - 1) [\hat{s}_i^+ \hat{s}_k^+ + \hat{s}_i^- \hat{s}_k^-] \right), \quad (4)
\end{aligned}$$

where the angles $\varphi_{i,j} \equiv \delta_j - \delta_i$, $\varphi_{i,k} \equiv \delta_k - \delta_i$ between two nearest-neighbor and next-nearest-neighbor spins are $\varphi_{i,j} = \pi + \phi$, $\varphi_{i,k} = -2\phi$, respectively, and $s^\pm \equiv s^x \pm is^y$ are spin raising and spin lowering operators.

The ket and bra GS's $|\Psi\rangle$ and $\langle\Psi|$ of H are parametrised within the CCM as follows:

$$\begin{aligned}
H|\Psi\rangle &= E|\Psi\rangle; \quad \langle\tilde{\Psi}|H = E\langle\tilde{\Psi}|; \\
|\Psi\rangle &= e^S|\Phi\rangle; \quad S = \sum_{I \neq 0} \mathcal{S}_I \mathcal{C}_I^+; \\
\langle\tilde{\Psi}| &= \langle\Phi|\tilde{S}e^{-S}; \quad \tilde{S} = 1 + \sum_{I \neq 0} \tilde{\mathcal{S}}_I C_I^-.
\end{aligned} \quad (5)$$

The correlation operators S and \tilde{S} contain the correlation coefficients \mathcal{S}_I and $\tilde{\mathcal{S}}_I$ which have to be determined. Using the Schrödinger equation, $H|\Psi\rangle = E|\Psi\rangle$, we can now write the GS energy as $E = \langle\Phi|e^{-S}He^S|\Phi\rangle$. After the notational rotation of the local axes of the quantum spins, the sublattice magnetization is given by $M = -1/N \sum_i^N \langle\tilde{\Psi}|s_i^z|\Psi\rangle$.

To find the ket-state and bra-state correlation coefficients \mathcal{S}_I and $\tilde{\mathcal{S}}_I$ we require that the expectation value $\bar{H} = \langle\tilde{\Psi}|H|\Psi\rangle$ is a minimum with respect to \mathcal{S}_I and $\tilde{\mathcal{S}}_I$, such that the CCM ket-state and bra-state equations are given by:

$$\begin{aligned}
\langle\Phi|C_I^- e^{-S} H e^S |\Phi\rangle &= 0 \quad \forall I \neq 0 \\
\langle\Phi|\tilde{S}e^{-S}[H, C_I^+]e^S|\Phi\rangle &= 0 \quad \forall I \neq 0.
\end{aligned} \quad (6)$$

The CCM formalism is exact if we take into account all possible multispin configurations in the correlation operators S and \tilde{S} , which is, however, in general impossible for a quantum many-body model. Hence, it is necessary to use approximation schemes in order to truncate the expansion of S and \tilde{S} in the Eqs. (5) in any practical calculation. The most common scheme is the LSUB n scheme, where we include only n or fewer correlated spins in all configurations (or lattice animals in the language of graph theory) which span a range of no more than n adjacent (contiguous) lattice sites.

TABLE I: Number of fundamental GS configurations of the LSUB n approximation for the Shastry-Sutherland model using the Néel state ($\phi = 0$) and the spiral state ($\phi \neq 0$) as the CCM reference state.

LSUB n	Néel state: $\phi = 0$	spiral state: $\phi \neq 0$
2	1	12
4	35	248
6	794	6184
8	20892	166212

To find all possible fundamental configurations which are different under the point and space group symmetries of both the lattice and the Hamiltonian, we use the lattice symmetries. The numbers of fundamental configurations may be further reduced by the use of additional conservation laws. For example, in the case of the Néel state ($\phi = 0$), the Hamiltonian of Eq. (1) commutes with the total uniform magnetization, $s_T^z = \sum_k s_k^z$ (the sum on k runs over all lattice sites). the GS lies in the $s_T^z = 0$ subspace, and hence we exclude configuration with an odd number of spins or with unequal numbers of spins on the two equivalent sublattices. For the spiral state we cannot apply this property because it is not an eigenstate of s_T^z . We calculate the fundamental configurations numerically, and the results of the numbers of LSUB n configurations for $n \leq 8$ are given in Table I. By using parallel computing we are able to solve the 20892 equations of the CCM-LSUB8 approximation for the Néel reference state. However, for the spiral state the current limitations of computer power allow then solution of the CCM equations up to LSUB6, only.

Since the LSUB n approximation becomes exact in the limit $n \rightarrow \infty$, it is useful to extrapolate the 'raw' LSUB n results to the limit $n \rightarrow \infty$. Although an exact scaling theory for the LSUB n results is not known, there is some empirical experience^{18,19,20} how the physical quantities for antiferromagnetic spin models scale with n . As stated above for the Néel reference state we are able to calculate the GS energy E and the sublattice magnetization M within LSUB n up to $n = 8$. In order to obtain more accurate results for the GS energy, we now employ a scaling law^{19,20} in order to extrapolate our results in the limit $m \rightarrow \infty$, where

$$E(n) = a_0 + a_1 \frac{1}{n^2} + a_2 \left(\frac{1}{n^2} \right)^2. \quad (7)$$

We use CCM results for $n = 4, 6, 8$ in order to carry out these extrapolations.²⁰ We find, however, that other scaling laws proposed in the literature yield very similar results for the energy. In the Néel ordered phase we utilise²⁰ a scaling law with leading power $1/n$, i.e.,

$$M(n) = b_0 + b_1 \frac{1}{n} + b_2 \left(\frac{1}{n} \right)^2. \quad (8)$$

We find that this prescription again leads to reasonable results²⁰. However, applying this scaling rule to systems

showing an order-disorder transition at zero temperature this kind of scaling tends to overestimate the magnetic order and yields too large critical values for the exchange parameter driving the transition^{19,23}. The reason for that might consist in the change of the scaling near a critical point. Hence in addition to the scaling rule (8) we also use a leading 'power-law' scaling²⁰, given by

$$M(n) = c_0 + c_1 \left(\frac{1}{n} \right)^{c_2}. \quad (9)$$

The leading exponent c_2 is determined directly from the LSUB n data.

IV. RESULTS

We start with the discussion of the onset of the spiral phase in the quantum model. We calculate the GS energy as a function of J_2 using as reference state a spiral state as sketched in Fig. 1. As quantum fluctuations may lead to a "quantum" pitch angle that is different from the classical case, we consider the pitch angle in the reference state as a free parameter. We then determine the "quantum" pitch angle ϕ_{qu} by minimizing $E_{\text{LSUB}m}(\phi)$ with respect to ϕ in each order n . As for

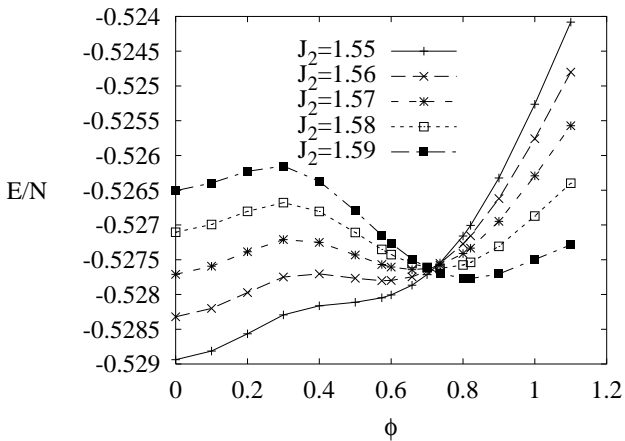


FIG. 2: Ground-state energy versus the pitch angle ϕ within CCM-LSUB4 approximation for different values of J_2 in the range $1.55 \leq J_2 \leq 1.59$.

the classical model for small J_2 the energy $E_{\text{LSUB}m}(\phi)$ has its minimum at $\phi_{qu} = 0$, i.e., the quantum GS is the semi-classical collinear Néel state. Contrary to the classical case, this collinear quantum state can survive into the region $J_2 > J_1$, where classically it is already unstable. This effect is known as *order from disorder*^{37,38} and is widely observed in quantum spin systems, see, e.g., Refs. 19,36. For frustrating couplings $J_2 \gtrsim 1.5J_1$ apart from the minimum at $\phi = 0$ a second minimum at a finite $\phi > 0$ emerges, which becomes the global minimum for strong enough J_2 . This scenario illustrated in Fig. 2 is

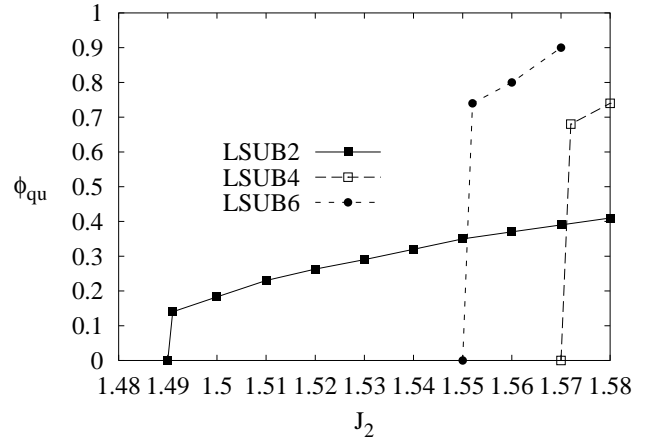


FIG. 3: The "quantum" pitch angle ϕ_{qu} as a function of J_2 calculated within CCM-LSUB n approximation with $n = 2, 4, 6$.

typical for a first-order transition, i.e., we find indications that quantum fluctuations may change the nature of the phase transition between the the collinear Néel phase to the noncollinear spiral phase from a second-order classical transition to a first-order quantum transition. Note that a similar situation can be found in other frustrated spin systems^{19,21}. The "quantum" pitch angle ϕ_{qu} , where $E_{\text{LSUB}m}(\phi)$ has its global minimum, is shown in Fig. 3. ϕ_{qu} shows a typical jump from $\phi_{qu} = 0$ to a finite value. Our data clearly indicate that the quantum noncollinear spiral phase has lower energy than the collinear phase only for strong frustration $J_2 \gtrsim 1.5J_1$.

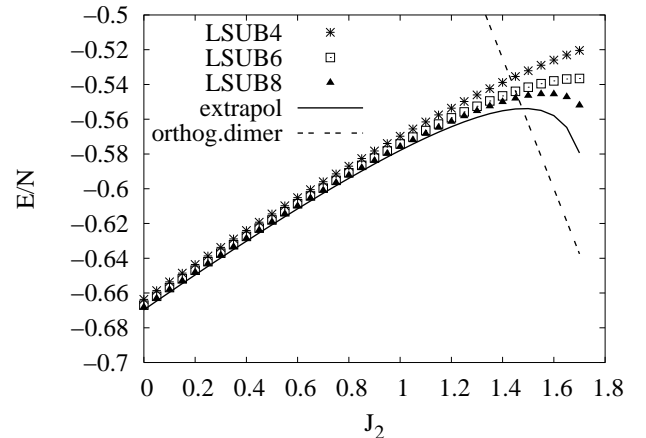


FIG. 4: The energy of (i) the collinear Néel phase as function of J_2 obtained by CCM-LSUB n with $n = 4, 6, 8$ and its extrapolated value to $n \rightarrow \infty$, see Eq. (7), and (ii) of the orthogonal-dimer state.

Next we consider the orthogonal-dimer state $|\Psi\rangle_{\text{dimer}}$ and compare its energy with that of the collinear Néel phase, see Fig 4. Our results demonstrate, that the

orthogonal-dimer state has lower energy than the Néel phase for $J_2 \gtrsim 1.477J_1$. $|\Psi\rangle_{\text{dimer}}$ remains the state of lowest energy also in the region where the noncollinear spiral state has lower energy than the Néel phase. We conclude that there is no intermediate spiral phase in the quantum model. Our estimate of the critical value $J_2^d = 1.477J_1$ where the transition to the orthogonal-dimer phase takes place is in good agreement with other results, cf. Table 2 in Ref. 32.

So far we have discussed mainly the energy of competing GS phases. The last question we would like to discuss is the question of the stability of the Néel LRO in the frustrated regime. For that we calculate the order parameter (sublattice magnetization) M within the LSUB n approximation scheme up to $n = 8$ and extrapolate to $n \rightarrow \infty$ using two variants of extrapolation as described in Sect. III. The results are shown in Fig. 5. The extrapolated data clearly demonstrate that the LRO vanishes before the orthogonal-dimer state becomes the GS. The transition from Néel LRO to magnetic disorder is of second order. Hence we come to the second important statement that there exists an intermediate magnetically disordered phase. Within the used CCM scheme starting from the Néel reference state we are not able to discuss the nature of the magnetically disordered state preceding the orthogonal-dimer state.

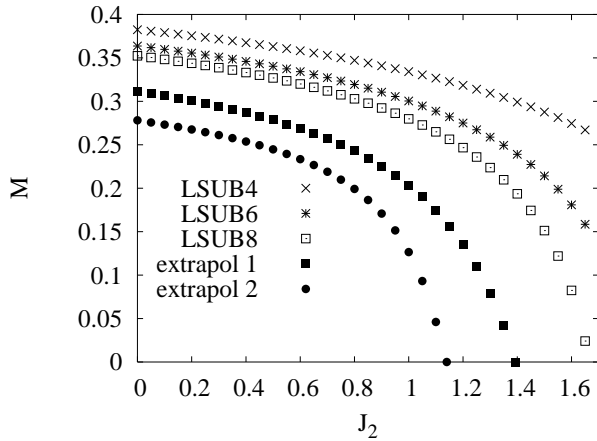


FIG. 5: Sublattice magnetization M versus J_2 obtained by CCM-LSUB n with $n = 4, 6, 8$ and its extrapolated values to $n \rightarrow \infty$ using two different extrapolation schemes, namely according to Eq. (8) (extrapol 1) and to Eq. (9) (extrapol 2).

Obviously, the critical value where J_2^c the Néel LRO breaks down depends on the used extrapolation formula. The extrapolation according to Eq. (8) leads accurate results for M in the unfrustrated ($J_2 = 0$) square-lattice limit and yields $J_2^c \sim 1.39J_1$. As discussed in Sect. III this extrapolation scheme tends to overestimate the region of magnetic LRO and indeed the value $J_2^c/J_1 = 1.39$ is significantly larger than the corresponding value calculated by series expansion, see Table 2 in Ref. 32. The extrapolation according to Eq. (9) is less accurate in the unfrustrated limit but yields a more reliable value $J_2^c \sim 1.14J_1$ which fits well to the corresponding value calculated by series expansion.

V. CONCLUSIONS

We have studied the GS phase diagram of the spin half Shastry-Sutherland antiferromagnet making use of high-order coupled cluster calculations. Comparing the energies of competing Néel, spiral and orthogonal-dimer phases we can rule out the existence of a noncollinear spiral phase. Considering the Néel order parameter we find that the semi-classical Néel long-range order disappears before the orthogonal-dimer phase sets in. Hence we conclude that the Néel phase and the dimer phase are separated by a magnetically disordered intermediate phase.

Acknowledgment: This work was supported by the DFG (project Ri615/12-1). The authors are indebted to the Rechenzentrum of the University Magdeburg and in particular to J. Schulenburg for assistance in numerical calculations.

¹ C. Lhuillier, P. Sindzingre, and J.-B. Fouet, Can. J. Phys. **79**, 1525 (2001).

² R. Moessner, Can. J. Phys. **79**, 1283 (2001).

³ G. Misguich and C. Lhuillier, *Two-dimensional quantum antiferromagnets*, \protect\url{http://arxiv.org/abs/cond-mat/0310405}, (2003).

⁴ J. Richter, J. Schulenburg, A. Honecker, in *Quantum Magnetism*, Lecture Notes in Physics **645**, U. Schollwöck, J. Richter, D.J.J. Farnell, R.F. Bishop, Eds. (Springer-Verlag, Berlin, 2004), pp 85 - 183 [http://www.tu-bs.de/~honecker/papers/2dqm.ps.gz].

⁵ P. Chandra and B. Doucot, *Phys. Rev. B* **38**, R9335 (1988).

⁶ H.J. Schulz and T.A.L. Ziman, *Europhys. Lett.* **18**, 355 (1992); H.J. Schulz, T.A.L. Ziman and D. Poilblanc *J. Phys. I* **6**, 675 (1996).

⁷ J. Richter, *Phys. Rev. B* **47**, 5794 (1993).

⁸ R.F. Bishop, *Phys. Rev. B* **58**, 6394 (1998).

⁹ O.P. Sushkov, J. Oitmaa, and Zheng Weihong, *Phys. Rev. B* **63**, 104420 (2001).

¹⁰ L. Capriotti, F. Becca, A. Parola, and S. Sorella, *Phys. Rev. Lett.* **87**, 97201 (2001).

¹¹ L. Capriotti, *Int. J. of Mod. Phys. B* **15**, 1799 (2001).

- ¹² B. S. Shastry and B. Sutherland, *Physica B* **108**, 1069 (1981).
- ¹³ H. Kageyama, K. Yoshimura, R. Stern, N.V. Mushnikov, K. Onizuka, M. Kato, K. Kosuge, C.P. Slichter, T. Goto, Y. Ueda, *Phys. Rev. Lett.* **82**, 3168 (1999)
- ¹⁴ S. Miyahara, K. Ueda, *Phys. Rev. Lett.* **82**, 3701 (1999).
- ¹⁵ M. Roger and J.H. Hetherington, *Phys. Rev. B* **41**, 200 (1990).
- ¹⁶ R.F. Bishop, J.B. Parkinson, and Y. Xian, *Phys. Rev. B* **44**, 9425 (1991).
- ¹⁷ R.F. Bishop, R.G. Hale, and Y. Xian, *Phys. Rev. Lett.* **73**, 3157 (1994).
- ¹⁸ C. Zeng, D.J.J. Farnell, and R.F. Bishop, *J. Stat. Phys.* **90**, 327 (1998).
- ¹⁹ S.E. Krüger, J. Richter, J. Schulenburg, D.J.J. Farnell and R.F. Bishop, *Phys. Rev. B* **61**, 14607 (2000).
- ²⁰ R.F. Bishop, D.J.J. Farnell, S.E. Krüger, J.B. Parkinson, J. Richter, *J. Phys. Condens. Matter* **12**, 6877 (2000).
- ²¹ S.E. Krüger and J. Richter, *Phys. Rev. B* **64**, 024433 (2001).
- ²² D.J.J. Farnell and R.F. Bishop, in *Quantum Magnetism*, Lecture Notes in Physics **645**, U. Schollwöck, J. Richter, D.J.J. Farnell, R.F. Bishop, Eds. (Springer-Verlag, Berlin, 2004), pp 307
- ²³ R. Darradi, J. Richter, and S.E. Krüger, *J. Phys.: Condens. Matter* **16**, 2681 (2004).
- ²⁴ M. Albrecht and F. Mila, *Europhys. Lett.* **34**, 145 (1996).
- ²⁵ Zheng Weihong, J. Oitmaa, C. J. Hamer, *Phys. Rev. B* **65**, 014408 (2001).
- ²⁶ A. Läuchli, S. Wessel, M. Sigrist, *Phys. Rev. B* **66**, 014401 (2002).
- ²⁷ Zheng Weihong, C. J. Hamer, J. Oitmaa, *Phys. Rev. B* **60**, 6608 (1999).
- ²⁸ E. Müller-Hartmann, R.R.P Singh, C. Knetter, G. S. Uhrig, *Phys. Rev. Lett.* **84**, 1808 (2000).
- ²⁹ A. Koga, N. Kawakami, *Phys. Rev. Lett.* **84**, 4461 (2000).
- ³⁰ M., Al Hajji, N. Guihery, J.-P. Malrieu, and B. Bouquillon, *Eur. Phys. J. B* **41**, 11 (2004).
- ³¹ C. H. Chung, J. B. Marston, and S. Sachdev, *Phys. Rev. B* **64**, 134407 (2001).
- ³² S. Miyahara, K. Ueda, *J. Phys.: Condens. Matter* **15**, R327 (2003).
- ³³ N.B. Ivanov, and J. Richter, *Phys.Lett.A* **232**, 308 (1997), J. Richter, N.B. Ivanov, and J. Schulenburg, *J. Phys.: Condens. Matter* **10**, 3635 (1998), J. Schulenburg and J. Richter, *Phys. Rev. B* **65** 054420 (2002).
- ³⁴ K. Ueda and S. Miyahara, *J. Phys.: Condens. Matter* **11**, L175 (1999).
- ³⁵ A. Koga and N.Kawakami, *Phys. Rev. B* **65**, 214415 (2002).
- ³⁶ R. Bursill, G. A. Gehring, D. J. J. Farnell, J. B. Parkinson, T. Xiang, and C. Zeng, *J. Phys.: Condens. Matter* **7**, 8605 (1995)
- ³⁷ J. Villain, R. Bidaux, J.P. Carton, R. Conte, *J. Phys.* **41**, 1263 (1980)
- ³⁸ E.F. Shender, *Zh. Eksp. Teor. Fiz.* **83**, 326 (1982) (Sov. Phys. JETP **56**, 178 (1982))